

LITERATURE REVIEW OF OCEANIC TRANSFORMS

Senior Thesis

Submitted in partial fulfillment of the requirements for the

Bachelor of Science Degree

At The Ohio State University

By

Taylor Hollis

The Ohio State University

2017

Approved by

A handwritten signature in black ink, appearing to read 'm Barton', is written over a solid horizontal line.

Dr. Michael Barton, Advisor
School of Earth Sciences

TABLE OF CONTENTS

Abstract.....	ii
Acknowledgements.....	iii
List of Figures.....	iv
Introduction.....	1
Geologic Setting.....	2
Ocean Spreading	2
Methods	
Thermal Influence Methodology.....	4
Lithosphere Strength Methodology.....	4
Results.....	6
Summary and Conclusions.....	8
Suggestions for Future Research.....	11
References Cited.....	12

ABSTRACT

Ocean transform faults create segments of the mid-ocean ridge and rise systems. The transform morphology and offset are controlled by spreading rate, temperature, heat flow, and crustal strength. Numerical and analog modeling with modern computational power has made significant advances in the understanding of transforms. Heat distribution numerical modeling indicates that most heat is retained in the center of the transforms. In other modeling of oceanic transform faults, the greater part of the deformation made by the fault system to the ridge was in the center of the transform zone. The rheological properties of the mantle and crust is highly complex and hinders further numerical modeling with current computation power.

ACKNOWLEDGEMENTS

First, I would like to thank my fifth-grade math teacher, Mr. Hanzlik. Without his encouragement to broaden my interests into science and attend a physics summer camp for girls at The Ohio State University, I never would have fallen in love with the campus. Being a woman in science is difficult, and he gave me the confidence to pursue it despite the challenges that are still prevalent for women today. Next, I need to thank Dr. Karen Royce for her guidance that has led to an undying passion for Earth Science. She answered every question and calmed all anxieties about field camp. Thank you to Dr. Anne Carey who has pushed us all to be our best and helped us along the way.

I need to thank my friends who have put up with me for years. Not only do they understand my passions and education but encourage them. They are so intelligent, and I cannot wait to see where they go in life. They are always up for an adventure or help me out of a bind, or in one instance, a fence. I also need to thank my wonderful parents, Tim and Beth Hollis who go along with every whim. I have dragged them both to countless parks across the United States, and they have not complained once. Except that one time I spent two hours in the mineral exhibit at the Museum of Natural History. They are patient with a daughter who has a love of science and this planet. I would like to acknowledge my brother Daniel. We have a back and forth banter that is not like any other. He teases me incessantly about being the only one in the family not interested in business, but he still got me a geology pun mug as a present.

I want to thank Dr. Michael Barton for taking me on. His outgoing, welcoming personality has made me feel welcome. I also want to thank Jameson Scott for allowing me to work and help with this project. They both are so ardent about learning, understanding, and discovering. The School of Earth Sciences has become my family and to them I owe thanks for countless laughs, good times, and the niche they have created.

LIST OF FIGURES

1. Map showing the location of mid-ocean ridges from Macdonald (1982)
2. Figure showing the model setup from Dauteuil et al. (2002).
3. Figure showing the setup and comparison of putty arrangement in Dauteuil et al. (2002).
4. Graphs showing the thermal distribution along the transform from Behn et al. (2007).
5. Cross sections of the model results from Behn et al. (2007).
6. Figures showing the width of deformation in Dauteuil et al. (2002).
7. Figures comparing two transforms with different spreading rates (Dauteuil et al., 2002)
8. Graph plotting various oceanic transforms by spreading rate (Dauteuil et al., 2002).

INTRODUCTION

The ocean floor is still a mysterious place, but is becoming better known with modern technology advances. The oceanic crust is characterized by deep trenches and immense ridges of underwater mountains. These ridges are segmented by transform zones that are largely enigmatic in their origin since their proposed existence by Wilson (1965). Progress has been made since their discovery and development of ideas on the plate tectonic cycle. The orthogonal faults propagate in the direction of spreading creating strike slip motion between two adjacent parts of the crust with different ages (Gerya, 2012; Mauduit and Dauteuil, 1996).

Larger offsets produce a narrower zone of deformation and more orthogonal attitudes relative to the ridge crest (Mauduit and Dauteuil, 1996). Using plate tectonics and magnetic pole reversals, the original rift shape can be configured giving insight into the past bathymetry and processes of ridge segmentation. Buiter and Torsvik (2014) concluded that oceanic transform faults can form by the reactivation of sutures or old subduction zone shedding light onto previous tectonic settings.

With steep drop offs, transform faults not only alter the topography of the crust, but can alter the circulation pattern of oceans currents (Shannon and Chapman, 1991). The global effect of oceanic transforms on currents on a global scale is not widely understood, and this is an area of active research.

In this paper, I will review major characteristics of oceanic transforms based on observations and modeling. Future research directions will be recommended.

GEOLOGIC SETTING

Ocean Spreading

The mid-ocean ridge, or rise depending on the ocean, systems are a distinguishing feature of the Earth. A major part of the Wilson Cycle is characterized by ridges, at which new crust is created, offset by transform zones. At these constructive boundaries, there is crustal thinning (Macdonald et al., 1988). Although simplified, Figure 1 shows the expansive ridge system present on the ocean floor as proposed by Macdonald (1982).

The overall morphology of the ridge is partially controlled by the spreading rate, causing slow spreading ridges, like those in the Atlantic to form deep rift valleys (Macdonald, 1982). Intermediate and fast spreading ridges are distinguished by a high point (axial ridge) near the spreading axis and smooth descending limbs.

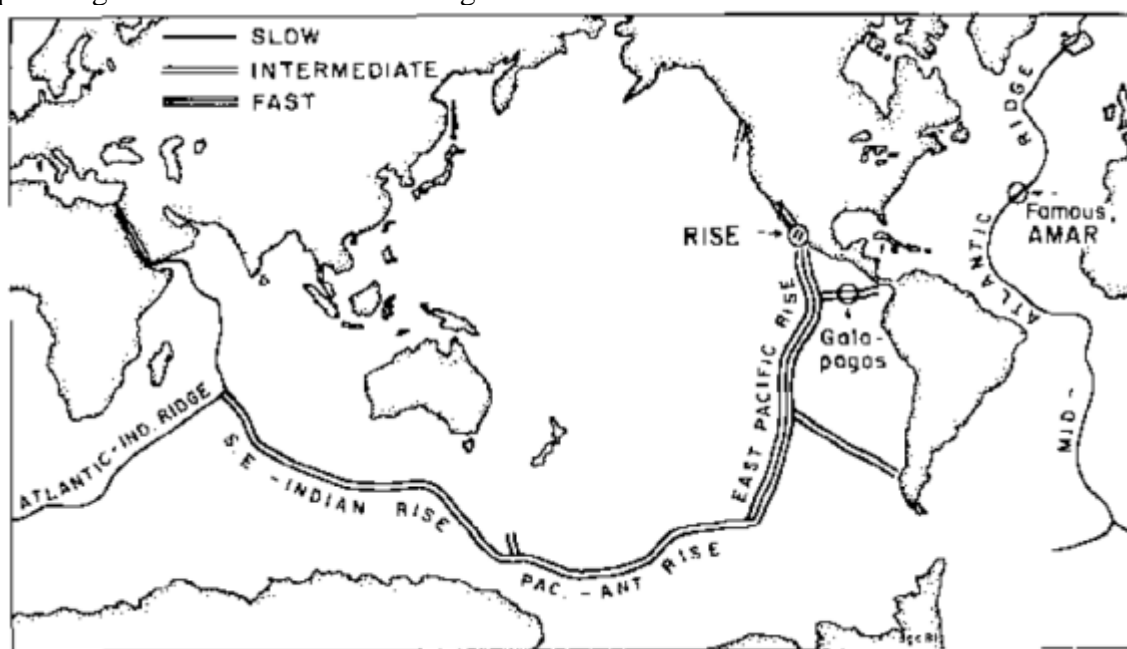


Figure 1: taken from Macdonald (1982); Map showing the ridge system on the ocean floor. The ridge or rise segments are denoted by their spreading rate. The highest accreting rises are in the Pacific

The uneven topography near the ridge axis can be credited to the result of volcanic activity (Ballard and Van Andel, 1977) and is typically 1–2 km wide (Ballard and Van Andel, 1977; Macdonald, 1982). Asymmetric spreading at the ridges is the result of asymmetric extensional forces pulling the crust apart (Macdonald, 1982). Axial depths and lithospheric thickness is affected by degree of asymmetric spreading of the ridges (Weatherly and Katz, 2010). The complexity of the mid-ocean ridge system adds to the mystery of oceanic transform faults that break the ridges into segments of varying length by the lateral offset. When a ridge is segmented, the two sections continue to “evolve independently” (Macdonald et al., 1988). This can result in asymmetrical spreading of the segments causing further offset on the transforms (Macdonald et al., 1988).

This thesis will explore different models that have been developed to reproduce transform forms and characteristics and summarize conclusions about oceanic transform fault properties.

METHODS

Thermal Influence methodology

Modeling of transforms constitutes a complex problem involving many different variables (Gerya, 2012). In modern research, numerical computer modeling and wax models are the two most common approaches used to understand these large and numerous features. The most important factor controlling transforms is the thermal relationship with the mantle (Behn et al., 2007). Four numerical models with different assumptions were explored by Behn et al. (2007). Equation 1 below was used by Behn et al. (2007) to calculate the dependence of viscosity on temperature. All models followed a 100 km deep scenario across a 150 km transform fault but different in other variables for model 1 viscosity was held constant, in model 2 viscosity was variable depending on temperature, model 3 had a temperature dependent viscosity with a fault, and model 4 had a correction for friction and a maximum viscosity (Behn et al., 2007).

$$\eta = \eta_0 \exp\left[\frac{Q_0}{R} \left(\frac{1}{T} - \frac{1}{T_m}\right)\right] \quad (1)$$

In equation 1, η represents temperature-dependent viscosity, η_0 is a constant 10^{19} Pa·s (viscosity of normal mantle), R is the gas constant, and Q_0 is the activation energy (250 kJ/mol) chosen for the model (Behn et al., 2007). In model 3, an area with a width of 5 km was weakened to create a brittle zone targeted for fault deformation (Behn et al., 2007). This area was modeled with a lower viscosity. Lower viscosities allow for increased mantle upwelling (Behn et al., 2007). In model 4, produced by Behn et al. (2007), accounted for “visco-plastic rheology” using equation 2 and a maximum viscosity.

$$\tau_{max} = C_0 + \mu \rho g z \quad (2)$$

In equation 2, C_0 is defined as cohesion, z as depth, g as acceleration due to gravity, ρ as density, and μ as the coefficient of friction (Behn et al., 2007). Without the predefined fault zone, a larger area is subject to deformation.

Lithosphere Strength methodology

In an experiment carried out by Dauteuil et al. (2002) producing a physical model, oceanic spreading boundaries were simulated by superimposing a brittle layer over a ductile layer representing the rheologically different layers of the lithosphere. The brittle layer was represented as sand, and silicone putty was used to for the viscous layer (Dauteuil et al. 2002). As illustrated in Figure 2, the starting length of the transform was 25 cm before the alterations and deformation caused in the experiment. The putty was spread over two different areas simulating different conditions within the crust. Three different conditions were tested including no putty (FT1), thin wedge of putty in a small area (FT2), and finally a wedge of putty over a larger area near the divergent zone and on the transform zone (FT3) as shown in Figure 2 (Dauteuil et al. 2002). These physical models were non-accretion of crust models meaning there was no addition of material to the spreading axis or transform. The spreading rate used in each experiment was 4 cm hr^{-1} and stopped when an offset of 2cm was reached (Dauteuil et al. 2002). At 4 cm hr^{-1} , this spreading rate is very rapid compared to real-world ridge spreading rates (Müller et al. 2008).

Similar experiments were performed by Marques et al. (2007) investigating crustal response and deformation to spreading. Similar to the experimental set-up of Dauteuil et al. (2002), in the fifth model considered by Marques et al. (2007), a putty of polydimethylsiloxane (PMDS) was used to line a preformed transform. The ridges were separated for 90 minutes and there was continual offset on the transform (Marques et al. 2007).

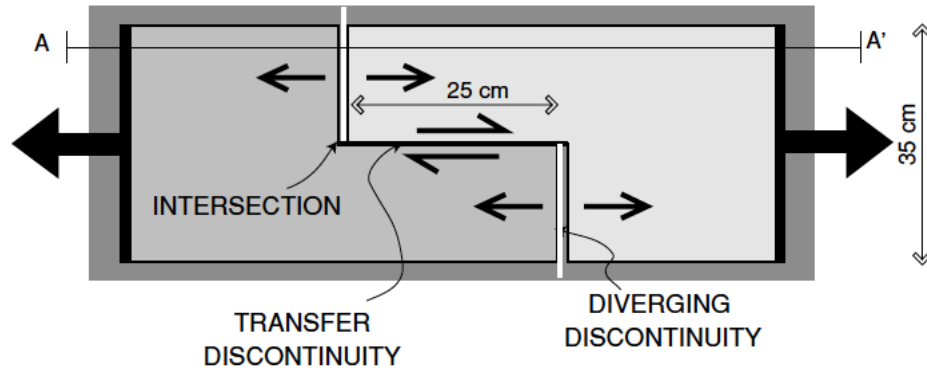


Figure 2: from Dauteuil et al. (2002); This figure shows a schematic of the top view experiment. The divergence was produced by pulling the two sheets away in opposite directions.

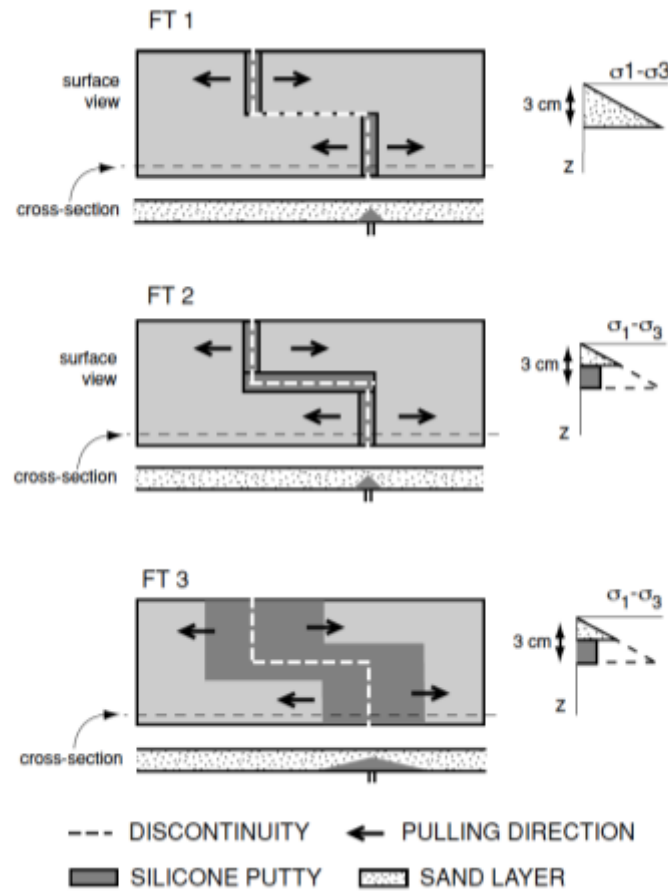


Figure 3: from Dauteuil et al. 2002; A basic overview of the setups showing the putty arrangement differences.

RESULTS

Thermal Structure

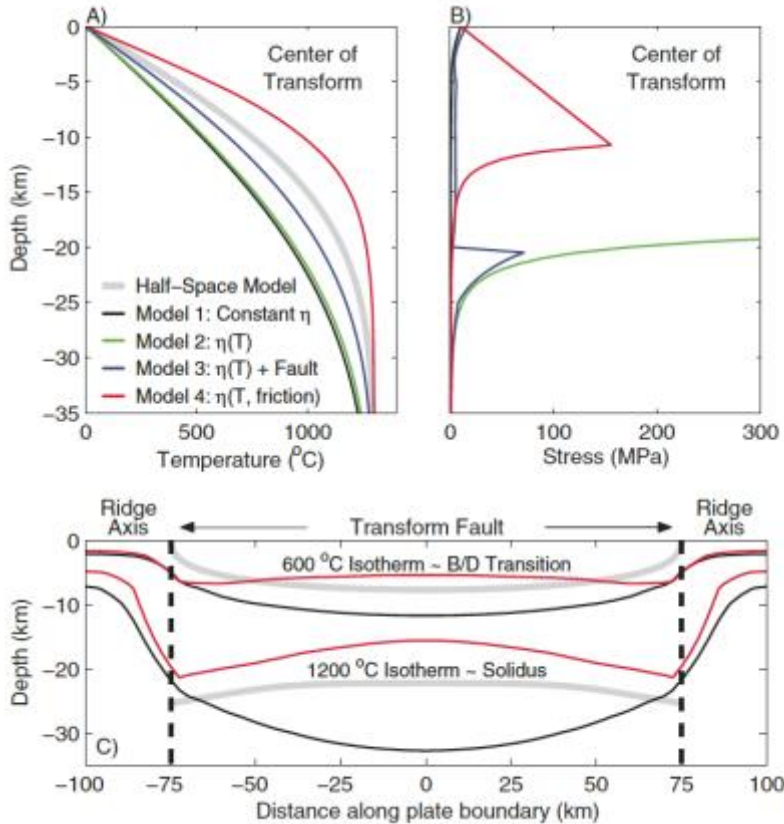


Figure 4: from Behn et al. (2007). (A) Graph showing the relationship between depth and temperature at the center of the transform. Graph B shows the magnitudes stress relative to depth at the center of the transform. The bottom figure is a cross section illustrating the 600 $^{\circ}\text{C}$ and 1200 $^{\circ}\text{C}$ isotherms position across the transform connecting the two ridge segments.

In the models calculated and produced by Behn et al. (2007), the distribution of heat across the transform boundary was represented in four ways. The temperature was highest in the center of the transform in models 3 and 4 shown in Figure 5 (Behn et al. 2007). The 600 $^{\circ}\text{C}$ isotherm was noticeably closer to the surface than predicted with the half-space model as was the 1200 $^{\circ}\text{C}$ isotherm in the center of the transform shown in Figure 4c. In models 1 and 2, the center of the transform has a lower temperature than that of models 3–4 but shows a greater distribution of the heat in the crust away from the ridge axis (Behn et al. 2007). In model 3, where viscosity was temperature dependent and there was a 5 km width of lower viscosity crust, there was a higher temperature distributed across the transform, but this model still closest relates to 1 and 2. The magnitude and temperature of heat upwelling in model 4 is

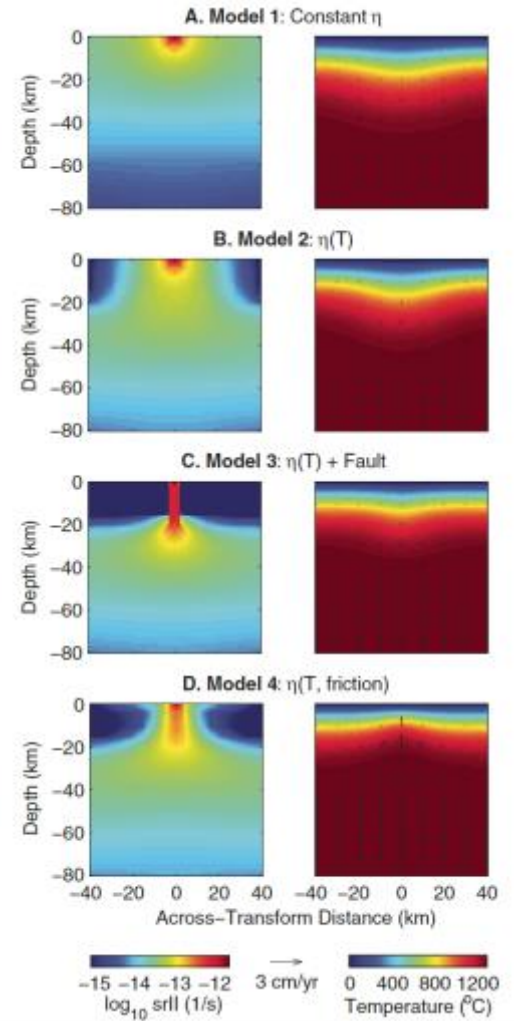


Figure 5: from Behn et al. (2007); Cross sections of 3D numerical experiments showing temperature distribution (right) and strain (left). Note significant difference in mantle upwelling in D.

visible in Figure 4D by Behn et al. (2007) showing cooling at the ridge terminations seen in natural transforms.

Deformation Structure

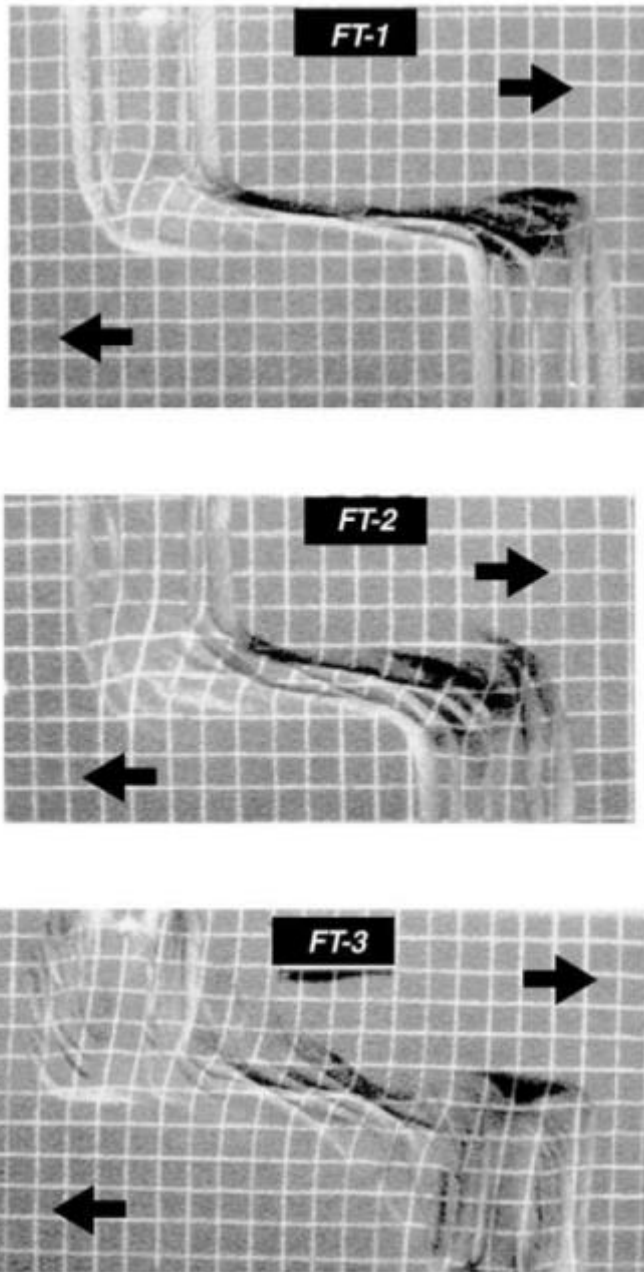


Figure 6: from Dauteuil et al. (2002) showing the different orientations of faults propagation in the experiment. The width of the deformation clearly differing from FT-1 to FT-2 to FT-3.

The different experiments produced superficially very similar looking results. In FT-1 shown in Figure 6 from Dauteuil et al. (2002), the deformation is defined by two oblique strike-slip faults almost parallel to the preformed transform. Normal faults are also formed and connect with the horizontal offsetting faults through what Dauteuil et al. (2002) call “horsetail pattern” faults. In comparison to FT-2 and FT-3, FT-1 produces deeper deformation, reaching 1.2 cm into the 3 cm deep sand (Dauteuil et al. 2002). FT-2 and FT-3 had deformation only reaching 0.8 cm and 0.7 cm, respectively (Dauteuil et al. 2002). The surface is more clearly distorted in the latter two models with widths of a few centimeters in the center of the transform (Dauteuil et al. 2002).

During the experiment conducted for FT-2 two sets of faults developed; the first set with trends 30° relative to the transform and the second set trending 15° relative to the transform (Dauteuil et al. 2002). This model also exhibits horsetail faults which produce the largest amount of vertical displacement (Dauteuil et al. 2002). During FT-3, the first set of faults propagating primarily altered the inside corners of the ridge-transform boundary (Dauteuil et al. 2002). The faults trend at a higher angle than that of the two previous models.

SUMMARY AND CONCLUSIONS

Spreading Rate

The attitude and form of oceanic transform faults depend on many properties. Important properties affecting the morphology of the fault include spreading rate and mantle viscosity (Gerya, 2010; Dauteuil et al., 2002; Weatherley and Katz, 2010). Gerya (2010) states that high viscosity mantle material produces high angle faults. High angle faults are more orthogonal to the ridge direction. Slow spreading ridges are dominated by transform zones that are narrow, deep, and likely to fill with sediments as shown in Figure 7 (Dauteuil et al., 2002). Fast spreading ridges as seen in the Pacific on the East Pacific Rise (EPR), have wider transform zones as is also shown in Figure 7 (Dauteuil et al., 2002; Gerya, 2012). Dauteuil et al. (2002) found that the Tjörnes Fracture Zone in the northern Atlantic has a significantly wide deformation zone for the spreading rate and segment length. This fracture zone lies on top of a hot spot causing the area to be hotter and therefore weakening the crust (Dauteuil et al., 2002). The Tjörnes Fracture Zone is an outlier on the graph from Dauteuil et al. (2002) that illustrates the correlation between accretion rate and width of deformation (Figure 8). Crust that is younger

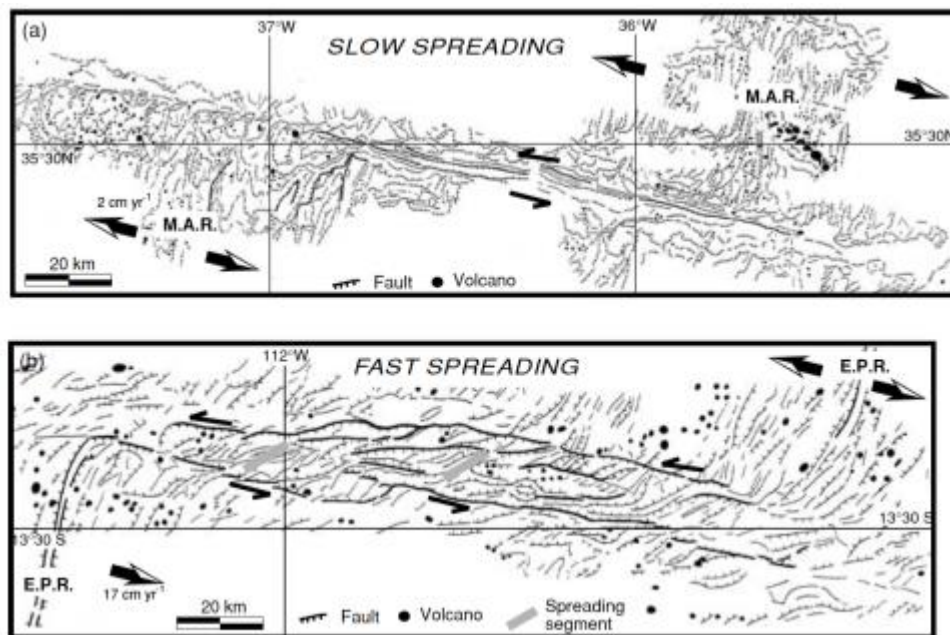


Figure 7: From Dauteuil et al. (2002), shows the differences of the deformation patterns depending on the spreading rate. The residual heat from the faster accreting ridges weaken the lithosphere allowing for a larger area of deformation.

Azores fracture zone (Dauteuil et al, 2002).

Spreading rate also has other effects on oceanic transforms. Spreading rate of the ridge is related to the segment length (Fox and Gallo, 1984; Carbotte and Macdonald, 1994). In the Pacific, where spreading rates are on average higher than those in the Atlantic, the segments separated by transforms are hundreds of kilometers long (Fox and Gallo, 1984). Transform faults breaking up the Mid-Atlantic Ridge are discernibly more abundant and segment lengths are shorter (Fox and

is hotter consequently causing the crust to be weaker and distributing the deformation across a larger area (Dauteuil et al., 2002; Gerya, 2010; Behn et al., 2007). This agrees with the conclusion of Dauteuil et al. (2002) that the lithosphere is weaker when there is a viscous layer present as shown in their experiment. A similar explanation applies to the

Gallo, 1984; Carbotte and Macdonald, 1994). Spreading rate changes can cause transform faults to nucleate or cause offset (Gerya, 2012). Offsets on oceanic transform faults are different from those along continental transform faults like the San Andreas Fault (Behn et al., 2002). Oceanic transforms experience a larger amount of aseismic offset (Behn et al., 2002, 2007). Behn et al. (2002) found that only 5% of shear strain is released from locked, mechanically coupled segments. The remaining strain is thought to be released through aseismic creep or slow low-magnitude earthquakes (Behn et al., 2002). However, there are some transforms that produce earthquakes with larger magnitudes. The Charlie-Gibbs transform zone in the Atlantic has produced a series of relatively large earthquakes since 1923 (Aderhold and Abercrombie, 2016). In 2015, the Charlie-Gibbs set off a M_w 7.1 earthquake (Aderhold and Abercrombie, 2016). The

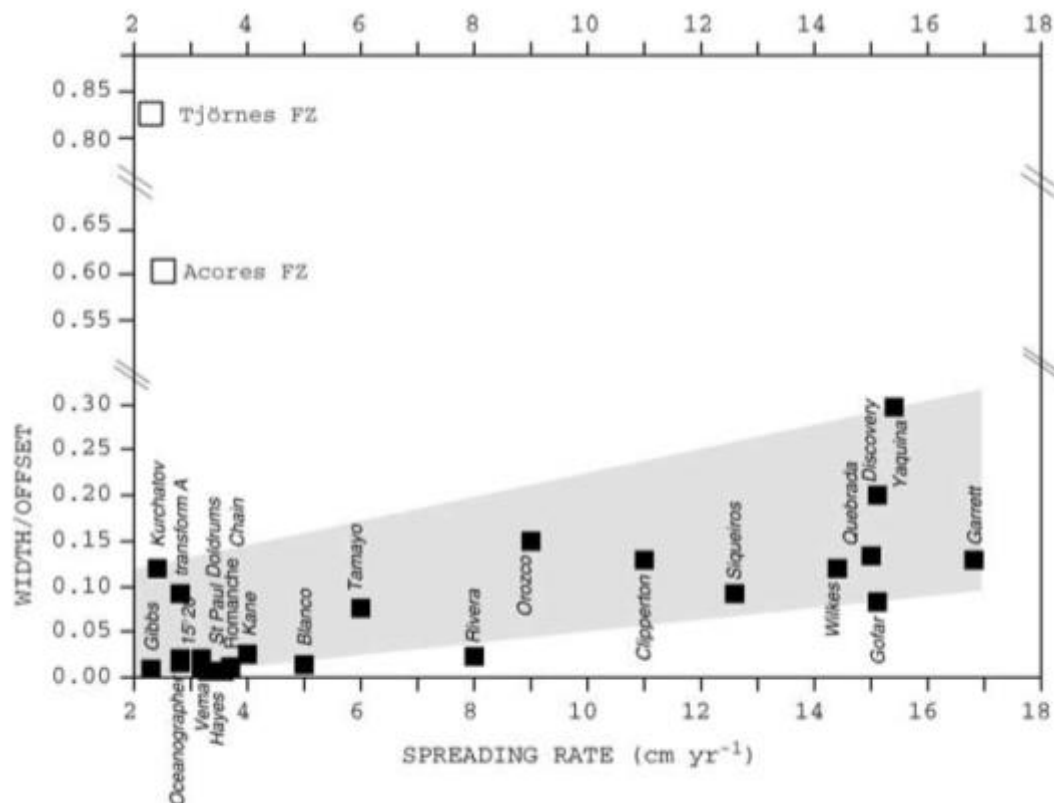


Figure 8: Taken from Dauteuil et al. (2002). Plots of various transform faults comparing spreading rate to width/offset.

Charlie-Gibbs is an outlier in terms of oceanic transform seismic activity.

Thermal Distribution and Morphology

The limbs of slow spreading ridges are cooler at a given distance from the ridge axis as they have greater ages. Transforms propagating from slower spreading ridges are more stable than those of faster accreting ridges (Mauduit and Dauteuil, 1996). This is because the deformation is focused on the center of the transform (Dauteuil et al., 2002), and the transforms hold the most heat in this central area due to increase mantle upwelling (Behn et al., 2007). As stated earlier, the warmer the lithosphere, the weaker it is. The rheology of the crust is controlled mainly by the temperature relating to the crustal thickness and magma injection (Behn et al., 2007). The

strength of the crust is constrained by the heat flow and composition (Dauteuil et al., 2002), while shape changes can be initiated by mantle dynamics and asthenospheric flow (Weatherly and Katz, 2010). The morphology of transform fault is very complex due to the three-dimensional variables of the asthenosphere, gravity, and rheology.

Oceanic Ridges spread at variable different rates, but the rates of those of the Atlantic cluster between two and four centimeters per year as illustrated in Figure 8 from Dauteuil et al. (2002). Ridge migration causes mantle upwelling and melting or an increase in temperature (Weatherly and Katz, 2010). This change causes the crust to weaken. The thermal distribution change, from the flow of the asthenosphere, across the transform fault then causes the deformation to be more wide-spread as seen in Figures 6 and 7.

RECOMMENDATIONS FOR FUTURE WORK

Transform faults are still a mysterious aspect of Earth Sciences. These large features below the ocean's surface affect plate tectonics and even ocean currents. With new technological advances, numerical modeling is becoming more sophisticated. Many unanswered questions remain to be researched on transform faults: What exactly causes transform fault nucleation? Does transform fault bathymetry cause other effects on ocean currents or ocean life? Can the geometry and attitude of a transform fault be controlled and predicted using different rheological and temperature variables? Does the Charlie-Gibbs have a higher fault coupling due to intratransform spreading? Does the Charlie-Gibbs have higher fault coupling from the reactivation of suture? How will the stability of oceanic transforms be affected by future seismic activity?

REFERENCES CITED

- Aderhold, K., & Abercrombie, R. E. (2016). The 2015 Mw 7.1 earthquake on the Charlie-Gibbs transform fault: Repeating earthquakes and multimodal slip on a slow oceanic transform. *Geophysical Research Letters*, 43(12), 6119-6128.
- Ballard, R. D., & van Andel, T. H. (1977). Morphology and tectonics of the inner rift valley at lat 36 50' N on the Mid-Atlantic Ridge. *Geological Society of America Bulletin*, 88(4), 507-530.
- Behn, M. D., Lin, J., & Zuber, M. T. (2002). Evidence for weak oceanic transform faults. *Geophysical Research Letters*, 29(24).
- Behn, M. D., Boettcher, M. S., & Hirth, G. (2007). Thermal structure of oceanic transform faults. *Geology*, 35(4), 307-310.
- Buiter, S. J., & Torsvik, T. H. (2014). A review of Wilson Cycle plate margins: A role for mantle plumes in continental break-up along sutures?. *Gondwana Research*, 26(2), 627-653.
- Carbotte, S. M., & Macdonald, K. C. (1994). Comparison of seafloor tectonic fabric at intermediate, fast, and super fast spreading ridges: Influence of spreading rate, plate motions, and ridge segmentation on fault patterns. *Journal of Geophysical Research: Solid Earth*, 99(B7), 13609-13631.
- Dauteuil, O., Bourgeois, O., & Mauduit, T. (2002). Lithosphere strength controls oceanic transform zone structure: insights from analogue models. *Geophysical Journal International*, 150(3), 706-714.
- Fox, P. J., & Gallo, D. G. (1984). A tectonic model for ridge-transform-ridge plate boundaries: Implications for the structure of oceanic lithosphere. *Tectonophysics*, 104(3-4), 205-242.
- Gerya, T. (2010). Dynamical instability produces transform faults at mid-ocean ridges. *Science*, 329(5995), 1047-1050.
- Gerya, Taras. (2012) "Origin and models of oceanic transform faults." *Tectonophysics* 522: 34-54.
- Macdonald, K. C. (1982). Mid-ocean ridges: Fine scale tectonic, volcanic and hydrothermal processes within the plate boundary zone. *Annual Review of Earth and Planetary Sciences*, 10(1), 155-190.
- Macdonald, K. C., P. J. Fox, L. J. Perram, M. F. Eisen, R. M. Haymon, S. P. Miller, S. M. Carbotte, M. H. Cormier, and A. N. Shor 9(1988). A new view of the mid-ocean ridge from the behaviour of ridge-axis discontinuities. *Nature*, 335(6187), 217-225.
- Marques, F. O., Cobbold, P. R., & Lourenço, N. (2007). Physical models of rifting and transform faulting, due to ridge push in a wedge-shaped oceanic lithosphere. *Tectonophysics*, 443(1), 37-52.
- Mauduit, T., & Dauteuil, O. (1996). Small-scale models of oceanic transform zones. *Journal of Geophysical Research: Solid Earth*, 101(B9), 20195-20209.

- Müller, R. D., Sdrolias, M., Gaina, C., & Roest, W. R. (2008). Age, spreading rates, and spreading asymmetry of the world's ocean crust. *Geochemistry, Geophysics, Geosystems*, 9(4).
- Shannon, L. V., & Chapman, P. (1991). Evidence of Antarctic bottom water in the Angola Basin at 32 S. *Deep Sea Research Part A. Oceanographic Research Papers*, 38(10), 1299-1304.
- Weatherley, S. M., & Katz, R. F. (October 01, 2010). Plate-driven mantle dynamics and global patterns of mid-ocean ridge bathymetry. *Geochemistry, Geophysics, Geosystems*, 11, 10.)
- Wilson, J. T. (1965). A new class of faults and their bearing on continental drift. *Nature*, 207, 343-347.